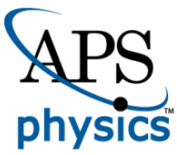

Operator growth and eigenstate entanglement in an interacting integrable Floquet system

Sarang Gopalakrishnan

Phys. Rev. B **98**, 060302 — Published 14 August 2018

DOI: 10.1103/PhysRevB.98.060302

Operator growth and eigenstate entanglement in an interacting integrable Floquet system

Sarang Gopalakrishnan
Department of Physics and Astronomy, CUNY College of Staten Island, Staten Island, NY 10314 and
Physics Program and Initiative for the Theoretical Sciences,
The Graduate Center, CUNY, New York, NY 10016

We analyze a simple model of quantum dynamics, which is a discrete-time deterministic version of the Fredrickson-Andersen model. This model is integrable, with a quasiparticle description related to the classical hard-rod gas. Despite the integrability of the model, commutators of physical operators grow with a diffusively broadening front, in this respect resembling generic chaotic models. In addition, local operators behave consistent with the eigenstate thermalization hypothesis (ETH). However, large subsystems violate ETH; as a function of subsystem size, eigenstate entanglement first increases linearly and then saturates at a scale that is parametrically smaller than half the system size.

Thermalization, decoherence, and information scrambling in isolated quantum systems are central themes in many-body physics [1–6]. Generic systems (except for the many-body localized phase [3, 4]) are believed to obey the eigenstate thermalization hypothesis (ETH), which posits that local observables in a many-body eigenstate behave as they would in an appropriately chosen thermal state [7–11]. However, many physically important one-dimensional systems (e.g., the Heisenberg spin chain) are integrable—i.e., they have extensively many conservation laws and hence do not thermalize [9, 12]. The absence of thermalization in integrable systems, and the slow "prethermal" relaxation of nearly integrable systems, have been experimentally observed [5, 13–17]. Some integrable systems can be mapped to free fermions [18], but others, including the Heisenberg chain, cannot [19]. In the latter class of "interacting" (i.e., Bethe-ansatz-solvable) integrable systems, it is challenging to compute the dynamics of physical observables, because physical operators have complicated representations in terms of the quasiparticles [20], although coarse-grained approaches to some dynamical questions have recently been developed [21–25]. In the quantum context, most work on integrable systems has focused on Hamiltonian dynamics, though there has been some recent work on time-periodic, driven integrable systems [26–28].

This work presents and analyzes a simple integrable Floquet model for which many of these questions can be explicitly addressed. This model is a deterministic discrete-time version of the Fredrickson-Andersen model [29–31], which is a standard model of kinetically constrained dynamics; we call it the Floquet-Fredrickson-Andersen (FFA) model. This model can be regarded as a block cellular automaton [32, 33], and its integrability as such was established in Ref. [32]. Dynamically, the FFA model resembles a classical hard-rod gas [24, 34], a canonical interacting integrable system; there is a natural description in terms of ballistically propagating quasiparticles. Beyond its integrability, what renders the model tractable is that its dynamics maps each computational-basis product state to a unique computational-basis product state; this allows for efficient classical simulations of dynamics. Despite its simplicity the FFA model retains two key features of generic integrable systems: first, the relation between physical observables and quasiparticles is nontrivial; and second, each quasiparticle's motion and available state space are modified by the distribution of other quasiparticles.

Our main results are as follows (Fig. 1). For physical observables the OTOC displays scrambling, with a front that broadens diffusively as expected for generic *chaotic* systems [35–42], but distinct from free-fermion systems [43]. However, the behavior *inside* the front is anomalous. In addition, small subsystems appear to satisfy ETH, in the sense that their reduced density matrices approach the identity, and the fraction of outlier states vanishes (slowly) in the thermodynamic limit, but large subsystems are strikingly nonthermal: for subsystem size $\gtrsim 2 \ln L$, the eigenstate entanglement crosses over from a thermal volume law to a constant. This crossover sharpens for larger systems.

Model.—The model we consider was recently introduced in Ref. [44]; the system is a spin-1/2 chain, subject

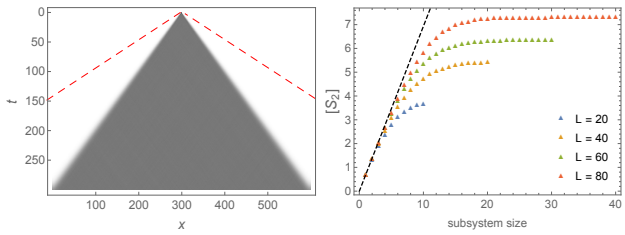

FIG. 1. Left: temporal growth of state-averaged out-of-time-order commutator for system size $L = 600$, averaged over 10000 initial states. Dashed red lines show the causal light-cone velocity, outside which the commutator strictly vanishes. Right: second Renyi entropy S_2 vs. subsystem size, averaged over 30 random eigenstates, for various system sizes L. Dashed black line has a slope of $\ln 2$, the thermal prediction. There is a clear crossover scale beyond which subsystem entanglement saturates.

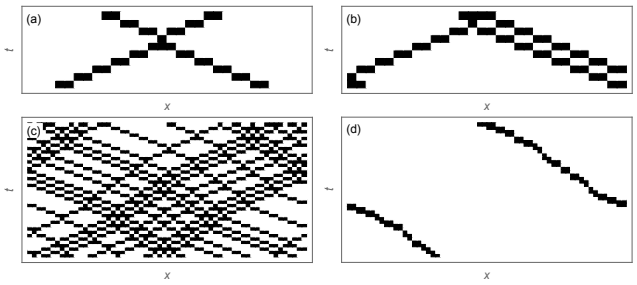

FIG. 2. Plots of spin dynamics; black cells are spin-up and white cells spin-down. (a) Collision of a right-moving and left-moving quasiparticle. (b) An initial state with four adjacent up spins is a three-quasiparticle state. (c) Time evolution of a product state in which the left and right third are generic, whereas the middle third has only one quasiparticle. (d) OTOC for this product state, obtained by moving one of the quasiparticles; note the absence of chaos.

to repeated application of the unitary

$$U = W(\text{odd} \to \text{even})W(\text{even} \to \text{odd}), \tag{1}$$

where $W(\text{even} \to \text{odd})$ consists of the following rule, applied to each odd spin n: apply the Pauli operator σ_n^x unless the two neighboring even sites, $n-1$ and $n+1$, are both in the $|\downarrow\rangle$ state. This rule can be composed from the gate sequence Toffoli$(n-1, n+1 \to n)$CNOT$(n-1 \to n)$CNOT$(n+1 \to n)$, in which controlled NOT and Toffoli gates are applied to the target site from its two neighbors. $W(\text{odd} \to \text{even})$ repeats this process with even and odd sites exchanged. The full-cycle unitary U has a strict causal light cone that expands at *two* sites per period (dashed red lines in Fig. 1). In what follows we treat periodic boundary conditions; the effects of other boundary conditions are deferred to future work. We also refer to odd (even) sites as the A (B) sublattices respectively.

Eq. (1) defines a reversible block cellular automaton [45, 46]. A number of works have addressed cellular automata and quantum circuits involving Clifford gates [35, 44, 47–49]. Clifford gates map each Pauli string to a unique Pauli string, and therefore do not give rise to operator entanglement [50, 51]. A related but Clifford-only model, without the Toffoli gate, was analyzed in Ref. [44] and shown to map to free particles. In contrast, the Toffoli gate in Eq. (1) induces operator entanglement for local operators, even after a single step of time evolution: for example, the operator σ_i^x evolves to $\tilde{\sigma}_i^x \equiv \frac{1}{16}(1+\sigma_{i-1}^x + \sigma_{i-2}^z - \sigma_{i-2}^z\sigma_{i-1}^x)\sigma_i^x(1+\sigma_{i+1}^x + \sigma_{i+2}^z - \sigma_{i+1}^x\sigma_{i+2}^z)$, which cannot be factored into on-site operators. Our methods here cannot be used to compute operator entanglement, however, so we defer a full discussion to future work.

Quasiparticle picture.—We first present a simple quasiparticle picture [32, 52] of the dynamics of this model. The structure of quasiparticles is easiest to describe when the density of up spins is low. In this limit, the elementary quasiparticles are pairs of two adjacent up spins surrounded by down spins. There are two inequivalent quasiparticles, respectively right- and left-moving, based on whether their sublattice structure is AB or BA. (The dynamics is symmetric under exchanging sublattices and time-translating by half a period, but not under each action separately.) All right-movers and all left-movers have the same speed, so collisions necessarily involve a right-mover and a left-mover; also, each three-body collision can only occur in one sequence, precluding diffractive processes. Each collision induces a time delay of one time step [Fig. 2(a)]; thus, this model resembles hard rods with *negative* rod length. The quantization condition for right (left) movers depends on the total number of left (right) movers. Since all quasiparticles have the same velocity, a state is characterized by *spacings* between adjacent left-movers (and between adjacent right-movers). Adjacent right-movers must have at least one empty site between them, since the configuration in Fig. 2(b) is not just a pair of right-movers; thus the state space is constrained, as in Ref. [53].

At finite density [Fig. 2(c)], the quasiparticle velocity decreases by an amount proportional to the density of other quasiparticles, which in turn is (approximately) proportional to the density of occupied sites; however, the dynamics still consists of ballistically moving quasiparticles. At high density, the model remains integrable. One can identify the quasiparticle content of a product state by recasting the model in terms of bonds [32], as follows [54]: assign a quasiparticle to each AB bond where both spins are up, and assign two quasiparticles to any spin configuration that has the sequence $\downarrow\uparrow\downarrow$. Note that the number of physical up spins fluctuates, though the number of quasiparticles remains conserved, because quasiparticles transiently "merge" during a collision [Fig. 2(a-b)]. The quasiparticle structure is explored further in [55], by simulating the "free expansion" [56] of a general initial state.

OTOCs.—The clearest evidence that the model remains integrable at high densities comes from studying OTOCs. In a classical system, the OTOC corresponds to the local overlap between two histories with identical initial conditions except for a disturbance at the origin [57]. For concreteness, consider the simplest OTOC, $C(x,t) \equiv \langle [X_0(0), Z_x(t)]^2 \rangle$. Expanding the commutator one finds the "out-of-time-order" term $ZXZX$, which can be written as $\langle\psi|Z_x(t)|\psi\rangle\langle\psi|X_0 Z_x(t) X_0|\psi\rangle$, where $|\psi\rangle$ is an arbitrary product state; evidently this quantity measures the overlap between the expectation value of $Z_x(t)$ in histories with an unperturbed initial state $|\psi\rangle$ and a perturbed initial state $X_0|\psi\rangle$. By expanding an arbitrary state in a product basis and keeping track of the phase accumulated, one can also compute generic OTOCs from this formula.

To establish integrability we perform the following numerical experiment [Fig. 2(c-d)]: we create an initial state with a region where the density of up spins in part of the system is low (so we can reliably create and ma-

nipulate a single quasiparticle there) but the rest of the system is at high density. We then move this quasiparticle, and overlap histories with different initial positions of the quasiparticle (i.e., we consider the OTOC $[Z_x(t), \sigma_0^+ \sigma^+ 1 \sigma_2^- \sigma_3^-]$). We find that translating a single quasiparticle does not have a "butterfly" effect: the OTOC is simply the time trace of the quasiparticle that was moved [Fig. 2(d)]. This indicates that the model remains integrable at high densities: in a chaotic system, "firing" a quasiparticle into the system at time time $t+\delta t$ rather than at t would cause a butterfly effect, which is clearly absent here.

Although moving quasiparticles does not cause a spreading disturbance, adding or removing quasiparticles does, as the presence of a new quasiparticle modifies the phase shifts of all the others. Physical spin operators create and/or move quasiparticles, depending on the underlying product state. All simple operators (i.e., those involving fewer than four sites) have matrix elements for both creating and translating quasiparticles: for instance, $\downarrow\uparrow\downarrow\uparrow\downarrow$ is a state with four quasiparticles, while $\downarrow\uparrow\uparrow\downarrow\downarrow$ is a state with only two quasiparticles. Therefore all such operators spread, although there exist operators acting on four or more sites [one example is $(1-\sigma_i^z)\sigma_{i+1}^+\sigma_{i+2}^+\sigma_{i+3}^-\sigma_{i+4}^-(1-\sigma_{i+5}^z)$ + h.c., which moves a quasiparticle one unit cell, but only if no other quasiparticles are in the way] that do not spread.

We now turn to the OTOC $[Z_x(t), X_0(0)]$ averaged over random basis states. (We have also checked the OTOCs of more complicated operators [55] but they do not behave appreciably differently, in contrast with the Ising case [43].) The OTOC averaged over many randomly chosen initial product states grows with a light-cone typical of chaotic systems (Fig. 1). The shape of the OTOC near its growth "front" matches the recent prediction for chaotic systems [36–40], with a tail that goes as $\exp[-(x-vt)^2/(2\sigma^2(t))]$, where $\sigma^2 \sim t$ [Fig. 3]. The velocity of the OTOC front is half the light-cone speed, since a random state is at half-filling. The FFA model is thus distinct from other large-N or "classical" limits, in which the OTOC front is sharp [35, 38, 39] (in the FFA model the front is sharp only if the initial state is a computational-basis product state). The diffusive broadening of the front here is a natural consequence of the random time delays due to collisions.

The late-time behavior of $C(x,t)$ has some unusual features, shown in the lower two panels of Fig. 3. Even at times before the operator has wrapped around the system, its behavior inside the front is athermal. Rather than decorrelating completely, the two histories remain weakly *anticorrelated* within the front (so the value of the OTOC inside the front is ≈ 0.53). This anticorrelation does not depend on system size. After a timescale $t \sim L/2$, this behavior changes and the two histories compared by the OTOC become weakly *correlated*, giving rise to the diamond-like shape seen in the space-time plot [Fig. 3, lower left]. The OTOC then saturates at a value ≈ 0.42 until the much longer revival timescale T_r.

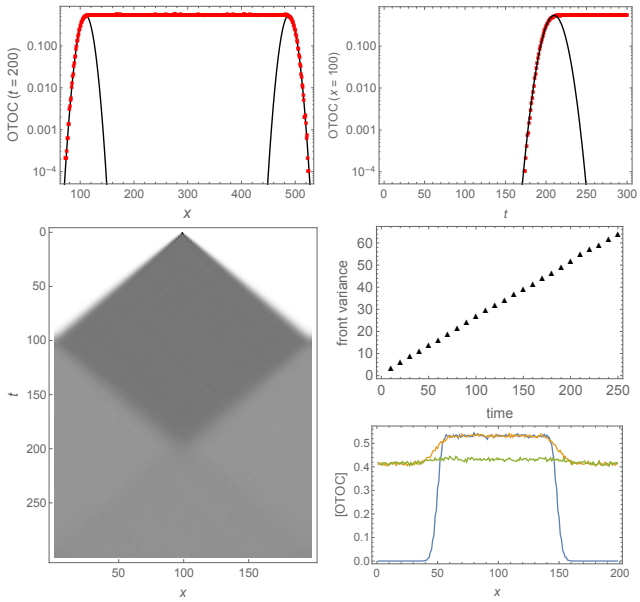

FIG. 3. Upper panel: Value of the OTOC at a fixed time, vs. position (left) and at a fixed position, vs. time (right), for $L = 600$ systems. The operator front is Gaussian. Middle right: squared width (variance) of operator front vs. time, indicating diffusive broadening. Lower left: density plot of the OTOC vs. time, for a smaller system ($L = 200$), showing the unexpected overshooting effect at times longer than system size; cross-sections at $t = 50, 100, 150$ are shown in the lower right panel.

These saturation values vary depending on the operator.

Our quantitative analysis of the OTOC involved averaging over eigenstates. The OTOC in a single randomly chosen eigenstate also spreads out with a broadened light-cone. However, the front "refocuses" on the timescale $t \sim L/2$ [55]. This can be understood within the quasiparticle picture. In a particular eigenstate, the distribution of left and right moving quasiparticles, and their spacings, are fixed, but one averages over the point in the trajectory at which the new quasiparticle is introduced. Thus, the sequence of time delays experienced by (say) a right-mover is randomized, but the total time delay is fixed by the total number of left-movers, causing refocusing at $t \propto L$. We expect Gaussian front-broadening at $t \ll L$, since on this timescale the average runs over randomly timed collisions.

Eigenstates.—We now turn to the eigenstates of the FFA model. Since U takes each product state to a product state, the dynamics of an initial product state consists of chains of transitions $|C_1\rangle \mapsto |C_2\rangle \mapsto |C_3\rangle \ldots \mapsto |C_N\rangle \mapsto |C_1\rangle \mapsto |C_2\rangle \ldots$. A random eigenstate can therefore be constructed [44] by picking a random initial product state and summing over its orbit, with appropriate phases, i.e.,

$$|E\rangle = \frac{1}{\sqrt{N}}(|C_1\rangle + e^{iq}|C_2\rangle + \ldots + e^{(N-1)iq}|C_N\rangle). \quad (2)$$

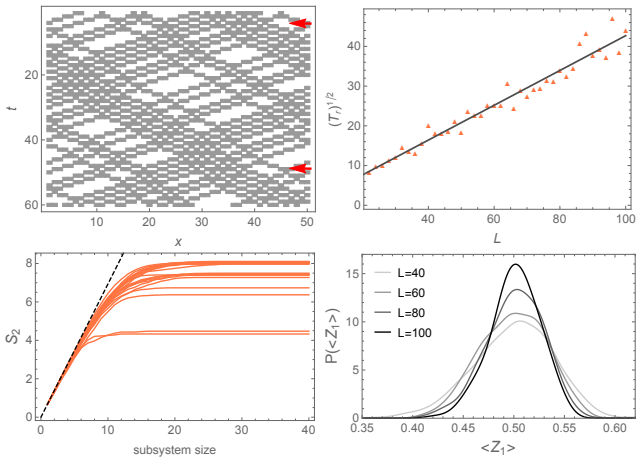

FIG. 4. Upper left: An example of the dynamics of an initial product state, illustrating how configurations recur after a period of order L up to an overall translation (see arrows; in this case the period is 45 and the shift is four sites to the left). Upper right: typical $\sqrt{T_r}$ vs. system size, as predicted by the quasiparticle picture. Left: State-to-state fluctuations of Renyi entropy S_2, vs. subsystem size, for $L = 80$; each line represents a randomly chosen eigenstate. Dashed black line has a slope of $\ln 2$. Right: histogram of the expectation value of the spin on the first site, $\langle Z_1 \rangle$, across eigenstates, for various system sizes. The histograms narrow with increasing system size.

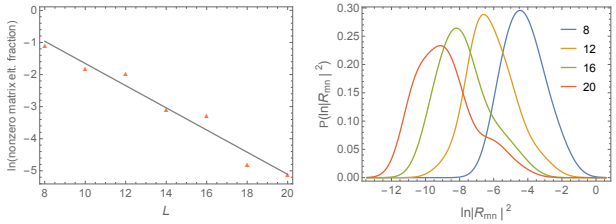

FIG. 5. Left: the fraction of nonzero off-diagonal matrix elements falls off exponentially with system size; the slope of the fit line is $-\ln 2/2$. Right: the distributions of the remaining nonzero matrix elements broaden (histograms are rescaled to have the same weight).

Such states are evidently eigenstates of U so long as $Nq = 2\pi n$ for some n.

A central quantity in our analysis is the recurrence time T_r for a given initial state, which measures how much of configuration space is accessible under unitary evolution from a given initial state. In an "ergodic" system (at least in the classical case relevant here), essentially every configuration would be visited, and T_r would grow exponentially with system size. This is not what happens in the FFA model (Fig. 4); instead $T_r \sim L^2$. This follows from the quasiparticle picture: a left-mover traverses the system on a timescale set by the number of right-movers, and vice versa. Since both numbers are of order L, their least common multiple is $\sim L^2$, although there are many configurations with a much smaller least common multiple, and for these T_r is much smaller.Note that T_r is a recurrence time specific to a particular initial computational-basis product state. The recurrence time of a random initial vector T_g is the least common multiple of each orbit's recurrence time. By sampling many initial states and computing their T_r, we find that this global recurrence time grows at least as fast as $T_g \gtrsim 4.8^L$ [55], so it is in general exponentially larger than the Hilbert space dimension. The quasiparticle picture also suggests that the scaling is exponential with system size: according to this picture, T_g is the least common multiple of all possible quasiparticle periods $\lesssim L$, which scales as the product of all primes $\lesssim L$; asymptotically this product grows exponentially in L by the prime number theorem. Thus, T_g scales exponentially rather than double-exponentially with system size, in contrast with generic chaotic models [50].

We previously showed [44] that $\ln T_r$ upper-bounds the second Renyi entanglement entropy S_2 [58] through any bipartite cut; an implication is that $S_2(\ell) \lesssim 2 \ln L$ for any subsystem size ℓ and system size L. This is what we find, by directly computing S_2 (Fig. 1). As Fig. 4 shows, there are strong state-to-state fluctuations in the saturation value of S_2, but the entanglement of every eigenstate saturates for subsystems well below half the system size. Small subsystems, on the other hand, are consistent with ETH: both S_2 and the expectation values of on-site operators are narrowly distributed, with state-to-state spread that narrows with system size (Fig. 4). This narrowing is slower than for generic ETH systems, however [55].

Eigenvalues and level statistics.—From the construction of eigenstates, it follows that each eigenvalue is of the form $\omega_n = 2\pi m/T_r^{(n)}, 0 \le m \le 2\pi T_r^{(n)}$, where n labels inequivalent orbits. There is an n-fold degeneracy at quasienergy zero (i.e., eigenvalue unity for the unitary U), as well as other degeneracies, so the level statistics are not Poisson or random-matrix.

Off-diagonal matrix elements.—Finally, we consider the off-diagonal matrix elements of local operators (specifically, the two-spin-flip operator $\sigma_i^x \sigma_{i+1}^x$) between eigenstates. We restrict ourselves to matrix elements between states in the quasi-energy zero sector. Most pairs of eigenstates have strictly zero matrix element; the fraction of nonzero matrix elements decreases exponentially with system size, approximately as $2^{-L/2}$ (Fig. 5). This behavior has also been seen in other integrable models [59]. The distribution of the nonzero matrix elements broadens with system size but does not seem to approach a Gaussian.

Discussion.—This work analyzed the FFA model, a simple interacting integrable Floquet system with a special basis in which the dynamics is classical. The FFA model is dynamically similar to a discretized hard-rod gas, except that the "rods" are dispersionless and thus all left-movers and right-movers have the same velocity. These simplifications make it possible to concretely ad-

dress many questions that are less tractable in other interacting integrable systems such as Heisenberg chains. As hard-rod gases are believed to be a general description of integrable dynamics [24], however, the present model *is* presumably a generic interacting integrable system in many respects. In this model, physical operators exhibit a butterfly effect, with a front that broadens diffusively as for chaotic systems [36, 37]. This feature (previously unnoticed [38, 40]) is presumably generic for interacting integrable systems, as it arises from the generic medium-dependence of quasiparticle velocities. Equilibrium density fluctuations exist at high temperature in all systems, and provided the quasiparticle velocities couple to these, the front should broaden diffusively. It remains to test this conjecture numerically, e.g., for Heisenberg chains.

Further, in the FFA model, the entanglement of small subsystems and *local* operators is consistent with ETH (which is nontrivial, given the classical dynamics of the model). However, large subsystems violate ETH: eigenstate entanglement has a sharpening crossover from volume-law growth to saturation, at a subsystem size that grows logarithmically with full system size. The level statistics and off-diagonal matrix elements of local operators also diagnose the non-thermal character of this model. Many questions remain for future work, including perturbations of the model that restore chaos and/or quantum fluctuations, as well as higher-dimensional generalizations.

ACKNOWLEDGMENTS

S.G. thanks David Huse, Vedika Khemani, Adam Nahum, Brian Swingle, and Romain Vasseur for helpful discussions and comments on a draft of this paper; Juan P. Garrahan for pointing out the work of Bobenko *et al.*; and Lincoln Carr, Andrew Potter, and Bahti Zakirov for helpful discussions on related topics. This work was supported by NSF Grant No. DMR-1653271.

[1] M. Cazalilla and M. Rigol, New Journal of Physics **12**, 055006 (2010).
[2] A. Polkovnikov, K. Sengupta, A. Silva, and M. Vengalattore, Rev. Mod. Phys. **83**, 863 (2011).
[3] D. Basko, I. Aleiner, and B. Altshuler, Annals of Physics **321**, 1126 (2006).
[4] R. Nandkishore and D. A. Huse, Annual Review of Condensed Matter Physics **6**, 15 (2015).
[5] T. Langen, R. Geiger, M. Kuhnert, B. Rauer, and J. Schmiedmayer, Nature Physics **9**, 640 (2013).
[6] A. M. Kaufman, M. E. Tai, A. Lukin, M. Rispoli, R. Schittko, P. M. Preiss, and M. Greiner, Science **353**, 794 (2016).
[7] J. M. Deutsch, Phys. Rev. A **43**, 2046 (1991).
[8] M. Srednicki, Phys. Rev. E **50**, 888 (1994).
[9] M. Rigol, V. Dunjko, and M. Olshanii, Nature **452**, 854 (2008).
[10] H. Kim, T. N. Ikeda, and D. A. Huse, Phys. Rev. E **90**, 052105 (2014).
[11] A. Dymarsky and H. Liu, arXiv preprint arXiv:1702.07722 (2017).
[12] E. Ilievski, M. Medenjak, T. Prosen, and L. Zadnik, Journal of Statistical Mechanics: Theory and Experiment **2016**, 064008 (2016).
[13] T. Kinoshita, T. Wenger, and D. S. Weiss, Nature **440**, 900 (2006).
[14] M. Gring, M. Kuhnert, T. Langen, T. Kitagawa, B. Rauer, M. Schreitl, I. Mazets, D. A. Smith, E. Demler, and J. Schmiedmayer, Science , 1224953 (2012).
[15] Y. Tang, W. Kao, K.-Y. Li, S. Seo, K. Mallayya, M. Rigol, S. Gopalakrishnan, and B. L. Lev, Physical Review X **8**, 021030 (2018).
[16] S. Erne, R. Buecker, T. Gasenzer, J. Berges, and J. Schmiedmayer, arXiv preprint arXiv:1805.12310 (2018).
[17] C. Li, T. Zhou, I. Mazets, H.-P. Stimming, Z. Zhu, Y. Zhai, W. Xiong, X. Zhou, X. Chen, and J. Schmiedmayer, arXiv preprint arXiv:1804.01969 (2018).
[18] T. D. Schultz, D. C. Mattis, and E. H. Lieb, Reviews of Modern Physics **36**, 856 (1964).
[19] L. Faddeev, in *Fifty Years of Mathematical Physics: Selected Works of Ludwig Faddeev* (World Scientific, 2016) pp. 370–439.
[20] J.-S. Caux and P. Calabrese, Phys. Rev. A **74**, 031605 (2006).
[21] O. A. Castro-Alvaredo, B. Doyon, and T. Yoshimura, Phys. Rev. X **6**, 041065 (2016).
[22] B. Bertini, M. Collura, J. De Nardis, and M. Fagotti, Phys. Rev. Lett. **117**, 207201 (2016).
[23] V. B. Bulchandani, R. Vasseur, C. Karrasch, and J. E. Moore, Phys. Rev. B **97**, 045407 (2018).
[24] B. Doyon, T. Yoshimura, and J.-S. Caux, Phys. Rev. Lett. **120**, 045301 (2018).
[25] V. Alba and P. Calabrese, Proceedings of the National Academy of Sciences , 201703516 (2017); SciPost Physics **4**, 017 (2018).
[26] V. Gritsev and A. Polkovnikov, SciPost Physics **2**, 021 (2017).
[27] M. Vanicat, L. Zadnik, and T. Prosen, arXiv preprint arXiv:1712.00431 (2017).
[28] T. Ishii, T. Kuwahara, T. Mori, and N. Hatano, Phys. Rev. Lett. **120**, 220602 (2018).
[29] F. Ritort and P. Sollich, Advances in Physics **52**, 219 (2003).
[30] J. P. Garrahan, arXiv preprint arXiv:1709.09208 (2017).
[31] J. M. Hickey, S. Genway, and J. P. Garrahan, Journal of Statistical Mechanics: Theory and Experiment **2016**, 054047 (2016).
[32] A. Bobenko, M. Bordemann, C. Gunn, and U. Pinkall, Communications in mathematical physics **158**, 127 (1993).
[33] T. Prosen and C. Mejía-Monasterio, Journal of Physics A: Mathematical and Theoretical **49**, 185003 (2016).
[34] H. Spohn, *Large scale dynamics of interacting particles* (Springer Science & Business Media, 2012).
[35] A. Nahum, J. Ruhman, S. Vijay, and J. Haah, Phys.

Rev. X **7**, 031016 (2017).
[36] C. W. von Keyserlingk, T. Rakovszky, F. Pollmann, and S. L. Sondhi, Phys. Rev. X **8**, 021013 (2018).
[37] A. Nahum, S. Vijay, and J. Haah, Phys. Rev. X **8**, 021014 (2018).
[38] S. Xu and B. Swingle, arXiv preprint arXiv:1802.00801 (2018).
[39] S. Xu and B. Swingle, arXiv preprint arXiv:1805.05376 (2018).
[40] V. Khemani, D. A. Huse, and A. Nahum, arXiv preprint arXiv:1803.05902 (2018).
[41] D. Rowlands and A. Lamacraft, arXiv:arXiv:1806.01723 (2018).
[42] M. Knap, arXiv:1806.04686.
[43] C.-J. Lin and O. I. Motrunich, Phys. Rev. B **97**, 144304 (2018).
[44] S. Gopalakrishnan and B. Zakirov, arXiv preprint arXiv:1802.07729 (2018).
[45] B. Schumacher and R. F. Werner, arXiv preprint quant-ph/0405174 (2004).
[46] I. Lesanovsky, K. Macieszczak, and J. P. Garrahan, arXiv preprint arXiv:1804.09794 (2018).
[47] J. Gütschow, S. Uphoff, R. F. Werner, and Z. Zimborás, Journal of Mathematical Physics **51**, 015203 (2010).
[48] R. F. Werner, V. Nesme, and J. Gütschow, Discrete Mathematics & Theoretical Computer Science (2010).
[49] A. Chandran and C. R. Laumann, Phys. Rev. B **92**, 024301 (2015).
[50] P. Hosur, X.-L. Qi, D. A. Roberts, and B. Yoshida, Journal of High Energy Physics **2016**, 4 (2016).
[51] C. Jonay, D. A. Huse, and A. Nahum, arXiv preprint arXiv:1803.00089 (2018).
[52] C.-N. Yang and C. P. Yang, Journal of Mathematical Physics **10**, 1115 (1969).
[53] A. Chandran, M. D. Schulz, and F. J. Burnell, Phys. Rev. B **94**, 235122 (2016).
[54] D.A. Huse, private communication.
[55] See online supplemental material..
[56] M. Rigol and A. Muramatsu, Modern Physics Letters B **19**, 861 (2005).
[57] A. Das, S. Chakrabarty, A. Dhar, A. Kundu, R. Moessner, S. S. Ray, and S. Bhattacharjee, arXiv preprint arXiv:1711.07505 (2017).
[58] M. A. Nielsen and I. Chuang, *Quantum computation and quantum information* (AAPT, 2002).
[59] V. Khemani, private communication.